Structural Engineering and Mechanics, *Vol. 69, No. 1 (2019) 77-93*
DOI: https://doi.org/10.12989/sem.2019.69.1.077

Structural performance of recycled aggregates concrete sourced from low strength concrete

Caglar Goksu*, Ilyas Saribas[a], Ergun Binbir[a], Yılmaz Akkaya[b] and Alper Ilki[b]

Istanbul Technical University, Civil Engineering Faculty, Maslak, Istanbul, Turkey

(Received March 21, 2018, Revised November 20, 2018, Accepted November 22, 2018)

Abstract. Although much research has been carried out using recycled aggregates sourced from normal strength concrete, most of the buildings to be demolished are constructed with low strength concrete. Therefore, the properties of the concrete incorporating recycled aggregates, sourced from the waste of structural elements cast with low strength concrete, were investigated in this study. Four different concrete mixtures were designed incorporating natural and recycled aggregates with and without fly ash. The results of the mechanical and durability tests of the concrete mixtures are presented. Additionally, full-scale one-way reinforced concrete slabs were cast, using these concrete mixtures, and subjected to bending test. The feasibility of using conventional reinforced concrete theory for the slabs made with structural concrete incorporating recycled aggregates was investigated.

Keywords: bond; durability; flexural behavior; low strength concrete; recycled aggregate; reinforced concrete; slab; three-point bending test

1. Introduction

The awareness and concerns over environmental issues (such as the increase in the greenhouse gases in the atmosphere, carbon footprint etc.) shifted the approach of treating the use of recycled materials in construction as one of the waste reduction methods to value-added materials that can be continually reused. Furthermore, social and economic drivers changed the traditional production performance indicators, as they are now often complemented with sustainability indicators such as reuse, repair or recycle. From the perspective of the construction sector, concrete is one of the most available materials for recycling. This is because concrete is the most used man-made material worldwide, and the production, usage and elimination phases of concrete after the completion of structural service life suggest negative impacts on the environment and economy. Therefore, it is clear that efforts on recycling the concrete to obtain aggregates to be used in construction of new buildings would be beneficial in terms of both economy and environmental sustainability, especially in densely populated urban areas, by reducing both the need to deposit in landfills and demand for natural resources.

The use of demolition waste from concrete structures as an aggregate for new concrete production has been intensively studied in the past few decades (Hansen 1992, Khalaf and DeVenny 2004, Attaullah *et al.* 2013). It was reported that the replacement of natural aggregate (NA) with recycled concrete aggregate (RCA) decreased the compressive strength up to 25%, splitting and flexural tensile strength up to 10% and the modulus of elasticity up to 45% (Hansen 1992, Ajdukiewicz ve Kliszczewicz 2002, Limbachiya *et al.* 2004, Sanchez ve Gutierrez 2004, Rakshvir and Barai 2006, Rahal 2007, Yang *et al.* 2008, Yehia *et al.* 2008, Corinaldesi 2010, Malesev *et al.* 2010, Rao *et al.* 2011, Sim and Park 2011, Xiao *et al.* 2012, Garg *et al.* 2013, Vyas and Bhatt 2013). Besides the adverse effect on the mechanical properties, replacement of NA with RCA also increased the drying shrinkage, creep and water absorption of concrete up to 50% (Gomez 2002a and 2002b, Li 2008, Fathifazl *et al.* 2011, Henschen *et al.* 2012, Fathifazl and Razaqpur 2013, Palaniraj and Dhinakaran 2013, Xiao *et al.* 2014, Silva *et al.* 2015). Significant number of the existing reinforced concrete (RC) buildings in large cities have completed their economic life or have the risk of collapse or heavy damage during earthquakes. For example, due to scarcity of ready-mixed concrete plants, the RC frame buildings built between 1920s to 1990s in Turkey were constructed using poor quality concrete. Due to the substandard construction practices in the past, earthquakes have caused significant human life and property losses (Tapan *et al.* 2013, Ilki and Celep 2012). Recently urban transformation projects were started in Turkey, to demolish the old and damaged RC structures, and replace with new structures (Urban Transformation Act, 06/05/2012 - 6306). Two billion tons of demolition waste is expected to emerge with this urban transformation process within the next 20 years. The demolition waste will cause negative environmental impacts, and new building construction will notably increase the demand for NA. Therefore, recycling the demolition waste and using RCA obtained from this demolition waste in new concrete

*Corresponding author, Ph.D.
E-mail: goksuc@itu.edu.tr
[a]Ph.D. Candidate
[b]Professor

ISSN: 1225-4568 (Print), 1598-6217 (Online)

(a)

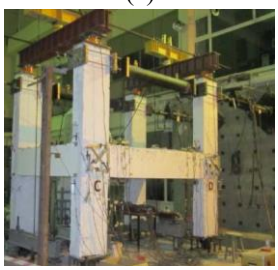

(b)

(c)

Fig. 1 (a) Recycled columns [35], (b) Recycled 3D frames [36], (c) Waste of recycled specimens

production would be the most convenient solution for reducing the waste to be landfilled and the demand for NA. For this purpose, an extensive experimental campaign was carried out to investigate the viability of using RCA as a suitable substitute for NA. According to the best knowledge of the authors, this is the first time that RCA was sourced from concrete structural members with concrete compressive strength values as low as 7 MPa. In the first phase of the study, tests were performed on RCA to determine its physical, chemical and durability characteristics. Based on these tests, only RCA with maximum size of 5-12 mm was considered as a suitable material for use in structural concrete. Later, four different concrete mixtures were designed incorporating NA and RCA. Two of the four concrete mixtures were designed using fly ash, as a pozzolanic material. In the second phase of the study, mechanical tests were performed for obtaining the compression, flexure, splitting tension and bond strengths of the specimens made with these concrete mixtures, cast with and without RCA. Ultrasonic pulse velocity (UPV) and rapid chloride ion permeability tests were also performed to investigate the porosity of these specimens. Based on the mechanical test results, it was found that the incorporation of RCA had slightly influenced the compression, flexural tensile, splitting tensile and bond strengths of concrete. In the last phase of the experimental study, twelve full-scale one-way slabs were constructed

Fig. 2 RCA (a) 0-5 mm, (b) 5-12 mm, (c) 12-22 mm

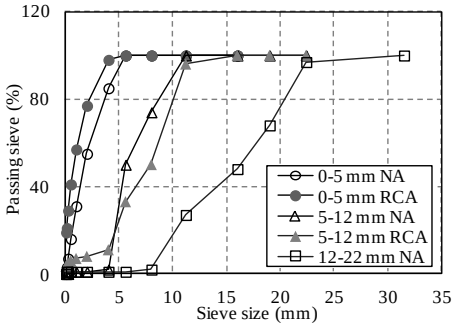

Fig. 3 Aggregate particle size distribution

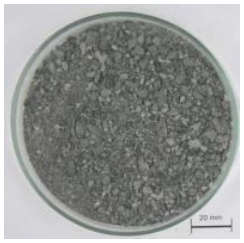

(a)

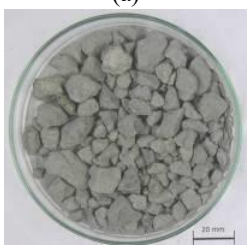

(b)

(c)

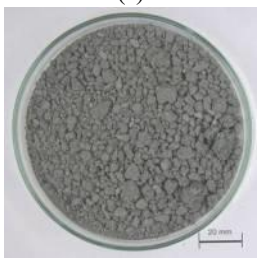

(d)

Fig. 4 0-5 mm RCA (a) Dry, (b) Washed and oven dry; 5-12 mm RCA (c) Dry, (d) Washed and oven dry

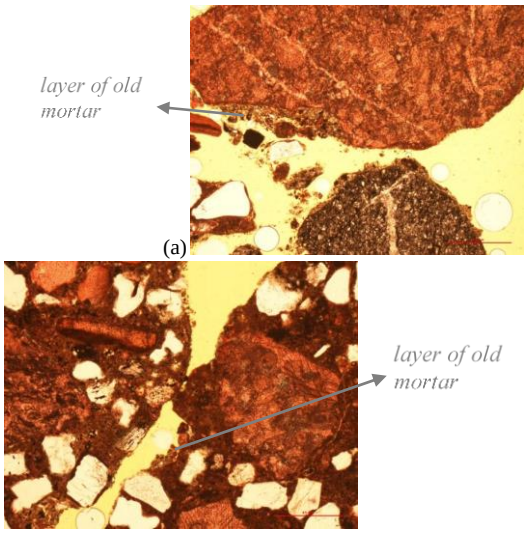

Fig. 5 Thin section photo with plane-polarized light, X50 (a) 0-5 mm RCA, with a layer of mortar bonded on the aggregate surface (b) 5-12 mm RCA, with chunks of sand particles embedded in the mortar

Table 1 Test results on NA and RCA

Aggregate tests	Standard	Unit	NA				RCA	
			Sand 0-2 mm	Crushed sand 0-5 mm	No 1 agg. 5-12 mm	No 2 agg. 12-22 mm	0-5 mm	5-12 mm
0.075 mm value	ASTM D 422	%	3.20	2.70	1.00	0.40	19	3.4
Water absorpt.	TS EN 1097-6	%	1.80	0.90	0.60	0.40	2.7	3.5
Particle density	TS EN 1097-6	g/cm^3	2.53	2.70	2.70	2.72	2.59	2.61
Chloride cont.	TS EN 1744-1	%	0.02	<0.001	<0.001	<0.001	<0.001	<0.001
Alkali cont.	ASTM C114-05	%	0.04	<0.01	<0.01	<0.01	<0.01	<0.01
Flakiness idx.	TS EN 933-3	%			11	5		
Shape idx.	TS EN 933-4	%			3	3		
Methylene blue	TS EN 933-9	%	0.5	<1	0.50	-	5.25	0.75
Los Angeles abr.	TS EN 1097-2	%	-	-	21	21	-	36
Org. impurities	TS EN 1744-1	-	Lighter	Lighter	Lighter	Lighter	Lighter	Lighter
Acid sol. sulp.	TS EN 1744-1	%	0.05	0.19	0.09	0.07	0.15	0.41
ASR	ASTM C1260	%	0.20	0.06	0.07	0.06	0.27	0.18
MS soundness	TS EN 1367-2	%	-	-	3	3	-	37
Shrinkage	TS EN 1367-4	%	0.044				0.05	

agg.: aggregate; abr.: abrasion; absorpt.: absoption; ASR: alkali silica reactivity; cont.: content; idx.: index; MS soundness: Soundness of Magnesium Sulphate; Org.: Organic; sol. sulp.: soluble sulphates

with the aforementioned concrete mixtures and subjected to bending tests for investigating whether the conventional RC theory is valid for the slabs made with structural concrete incorporating RCA. The slabs were selected as specimens to be tested for two main reasons: (i) The amount of concrete used in casting of slabs is much higher compared to columns and beams in practice. Therefore, in case the utilization of RCA in construction of slabs becomes mainstream, there would be a prompt reduction in the waste material storage. (ii) The concrete strength has only minor influence on the load-bearing capacity of flexural members, which are not subjected to axial forces. In literature, there are few studies on slabs incorporating RCA (Rao *et al.* 2012 and Rise *et al.* 2015, Francesconi *et al.* 2016, Schubert *et al.* 2012 and Michaud *et al.* 2016). Among these studies, research on flexural behavior of slabs is scarce (Xiao *et al.* 2015, Zhou *et al.* 2008) and do not cover the tests of members constructed using RCA sourced from low strength concrete. The results of the current study proved that the replacement of medium size coarse NA with RCA sourced from low strength concrete did not have adverse effects on the load bearing and deformation capacities of the slabs. Furthermore, an attempt was also made to predict the load-deflection relationships of the slabs numerically. The numerical analysis was performed using conventional RC theory and plastic hinge approach without any alteration for the slabs made with structural concrete incorporating RCA. It was found that the numerical model results in terms of load-deformation relationships were in compliance with the measured load-deflection curves up to high displacement levels.

2. Experimental work

2.1 Testing of RCA

In this study, the source of RCA is 10-year-old full scale laboratory test specimens, constructed according to traditional construction techniques and materials to resemble existing sub-standard structures. These structural elements were used for investigating the response of low strength concrete structures against seismic actions (Fig. 1). After testing, the structural elements were exposed to natural environmental conditions similar to the conventional structures (Cosgun *et al.* 2012, Ghatte *et al.* 2016). The concrete compressive strengths of these structural members ranged from 7 MPa to 16 MPa. To obtain RCA, these structural members were demolished, and then cleaned from extraneous materials and reinforcement by hand. No acid treatment was implemented during the cleaning process. Then the waste concrete was transported and crushed at an aggregate production plant using a jaw crusher and hammer mill crushers. Thereafter, the material was sieved into three fractions: 0-5 mm, 5-12 mm and 12-22 mm (Fig. 2). Fig. 3. presents the distribution of aggregate particle size of NA and RCA according to TS EN 933-1 (2012). As seen from this figure, the distribution of aggregate particle size of NA and RCA are similar to each other. The characteristics of RCA were then evaluated for their possible use in the production of new concrete mixtures. Based on the visual observations on RCA, significant amount of extraneous matters was found in 12-22 mm grade. Therefore, use of grade 12-22 mm was not considered in the production of new concrete mixtures. Macro visual observations on grades 0-5 mm and 5-12 mm are presented in Fig. 4. Petrographic analyses were also carried out on thin sections with a polarization microscope (Fig. 5). The amount of mortar bonded on RCA is also determined by microstructural studies, since it adversely affects the

strength of new concrete. Recycled aggregates included disseminated secondary micro quartz and euhedral secondary dolomite crystals, containing biomicritic and biomicrosparitic limestone. Fossil shells were generally filled with secondary calcite and with dolomite. Continuous and discontinuous veins were also filled with secondary calcite, dolomite, micro quartz and with pyrite. As it can be seen from Fig. 5, a layer of old mortar of the parent concrete can be seen around the aggregates. As reported previously by Poon *et al.* (2004) and De Brito *et al.* (2016), the old mortar is permeable and responsible for the poor bonding between the new cement paste and RCA.

The physical, chemical and durability tests performed on RCA and NA and the test results are listed in Table 1 for comparison. The density of RCA (2.61 g/cm^3) was lower than that of NA (2.70 g/cm^3) possibly due to remnants of the cement paste, bonded around the aggregates. This value for RCA is in accordance with the results reported in the literature, which provide density values as low as 2.46 g/cm3 [56] and 2.48 g/cm^3 (Thomas *et al.* 2016). The water absorption capacity, a distinct property that distinguishes RCA from NA, was higher in RCA (2.7% for 0-5 mm and 3.5% for 5-12 mm) than NA, possibly due to porous texture of the bonded remnant mortar. The higher water absorption capacity of RCA obtained in this study, is also comparable with the test results found in the literature, which varied between 4.19-5.61% (Tangchirapat *et al.* 2010, Ho *et al.* 2013, Thomas *et al.* 2016, Hasan *et al.* 2017).

As seen in Table 1, the value of materials passing from 0.075 mm sieve was found to be as high as 19% for RCA 0-5 mm grade. Since the finer size materials increase water demand of concrete, they adversely affect strength and permeability of concrete. In addition, short term accelerated alkali-aggregate reactivity mortar bar test result of 0-5 mm was higher than 0.2%, which indicates a higher risk for reactivity. As a conclusion, RCA 0-5 mm grade was also evaluated as an unsuitable material for use in structural concrete.

The Los Angeles abrasion of RCA was found to be 36%, higher than that of NA (21%). This result is comparable with the test results in the literature, which varied between 31-40% (Tangchirapat *et al.* 2010, Ho *et al.* 2013, Thomas *et al.* 2014). The higher Los Angeles abrasion of RCA than NA may be attributed to the adhered old cement mortar, which is usually weaker than NA (Shayan and Xu 2003). 5-12 mm grade RCA also presented alkali-aggregate expansion of less than 0.2%. Based on these test results, only the medium size fraction (5-12 mm) of RCA was used in the concrete production.

2.2 Testing of material properties of hardened concrete

Four different concrete mixtures were produced for testing the properties of concrete with and without RCA:

(i) M-R0: Mix with 100% NA,

(ii) M-R50: Mix with substitution of 50% of the coarse NA by RCA by weight,

(iii) M-R0-PZ: Mix with 100% NA and pozzolanic material (fly ash) (15% by cement weight),

(iv) M-R50-PZ: Mix with substitution of 50% of the coarse NA by RCA by weight and fly ash (15% by cement weight).

Table 2 Concrete mix-proportions*

Material quantity	M-R0	M-R50	M-R0-PZ	M-R50-PZ
NA-No 2 aggregate (10-20 mm) (kg)	489	493	472	472
NA-No 1 aggregate (5-12 mm) (kg)	501	-	484	-
RCA (5-12 mm) (kg)	-	522	-	500
Crushed sand (washed) (0-4 mm) (kg)	407	410	393	393
Sand (0-2 mm) (kg)	513	518	495	495
Fly ash (Class F) (kg)	-	-	50	50
Cement (CEM 42.5 R) (kg)	300	300	270	270
Water (lt)	128	110	142	131
Superplasticizer (Glenium ACE 450) (lt)	1.95	2.10	2.24	2.24
Water/Cement	0.43	0.37	0.49	0.45

*The intent of the study was to obtain similar concrete compressive strengths by using similar proportions of cement and different amounts of water considering the physical characteristics such as the high water absorption capacity of RCA with respect to NA.

Fly ash as a supplementary material in concrete has been used in concrete at levels ranging from 15% to 35% by mass of the cementitious material component. The actual amount that can be used varies widely, depending on the application, the properties of the fly ash, specification limits, and the geographic location and climate (Marceau *et al.* 2002, Thomas 2007). Due to its pronounced effects on the development of mechanical strength, 15% fly ash was used in this study.

Recycled aggregate is generally used as 10-35% replacement of coarse aggregate in the production of structural concrete (Gonçalves and De Brito 2009, Pacheco *et al.* 2013). In this study, No1 NA was completely replaced by RCA, which approximately corresponds to 50% replacement of the coarse aggregates. Although this ratio is higher than the currently suggested limits, it allowed to investigate the structural behavior of the slabs with higher RCA replacement ratios.

The compositions of the mixtures are presented in Table 2. Due to high water absorption capacity of RCA (Table 1), the water/cement ratios and admixture contents were adjusted to achieve similar workability for each concrete mixture. Achieving similar fresh concrete consistency was important to ensure similar compactibility performance. Slump test was implemented immediately after production of concrete and the results were obtained in the range of 18-22 mm (S4 Class).

Specimens were produced from each concrete mixture to investigate the effect of RCA and fly ash on the compressive strength, 3-point flexural tensile strength, splitting tensile strength and bond strength. Besides, UPV and electrical indication of concrete's ability to resist chloride ion penetration were performed on specimens produced from each mixture to investigate the effect of RCA and fly ash on porosity. At least three specimens were tested for each test.

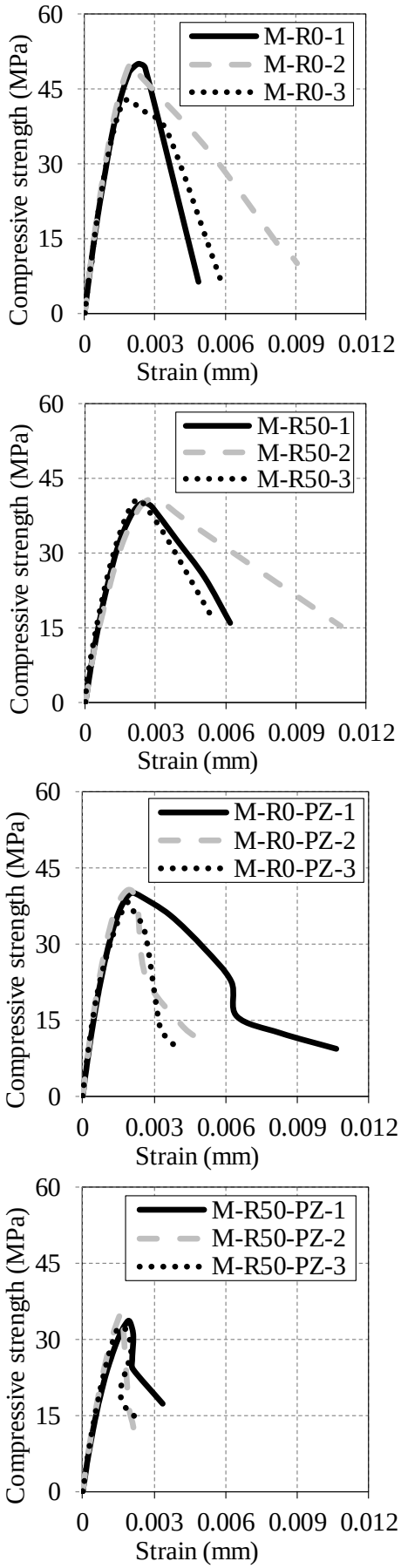

Fig. 6 Compressive strength-displacement relationships of the specimens

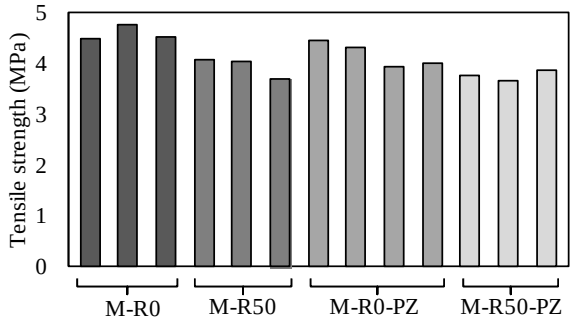

Fig. 7 Splitting tensile strengths of the specimens

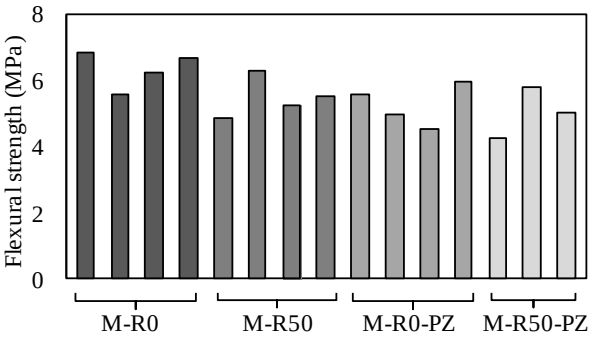

Fig. 8 Flexural strengths of the specimens

The compressive strength and splitting tensile strength were obtained based on the tests on cylinder specimens (150 mm×300 mm) (TS EN 12390-3 2002, TS EN 12390-6 2002). The 3-point flexural strength tests were conducted on 100 mm×100 mm×500 mm beam specimens in accordance with TS EN 12390-5 (2002). The tests results are presented in Figs. 6-8 and Table 3. Based on the average test results, the concrete compressive, splitting and flexural tensile strengths decreased with the incorporation of RCA. The decrease in concrete compressive, splitting tensile and flexural strengths of the group M-R50 with respect to the group M-R0 was 18%, 15% and 13%, respectively. These variations are attributed to the higher absorption capacity and poor interfacial transition zones between RCA and cement, as also previously reported by Lopez-Gayarre *et al.* (2009). The test results also revealed that partial replacement of cement with fly ash caused a decrease in concrete compressive, splitting tensile and flexural strengths. The decreases in the concrete compressive, splitting and flexural strengths of group M-R0-PZ with respect to the group M-R0 were 20%, 10% and 16%, respectively. The decreases in the concrete compressive, splitting tensile and flexural strengths of group M-R50-PZ with respect to group M-R50 were 17%, 4% and 9%, respectively. As expected from the aforementioned test results, the incorporation of both RCA and fly ash caused a decrease in concrete compressive, splitting tensile and flexural strengths. The decreases in the concrete compressive, splitting tensile and flexural strengths of group M-R0 with respect to the group M-R50-PZ were 31%, 18% and 20%, respectively.

The UPV was obtained based on the tests on cylinder specimens (150 mm×300 mm) (ASTM C597 2002). The

Table 3 Splitting tensile and flexural strengths of the specimens

Specimens	Splitting tensile strength (MPa)			Fexural strength (MPa)		
	Strength	Average	Standard deviation	Strength	Average	Standard deviation
M-R0-1	4.5	4.6	0.1	6.9	6.2	0.5
M-R0-2	4.8			5.6		
M-R0-3	4.5			6.2		
M-R0-4	-			6.7		
M-R50-1	4.1	3.9	0.2	4.9	5.5	0.6
M-R50-2	4.0			6.3		
M-R50-3	3.7			5.3		
M-R50-4	-			5.5		
M-R0-PZ-1	4.4	4.2	0.2	5.6	5.0	0.4
M-R0-PZ-2	4.3			5.0		
M-R0-PZ-3	3.9			4.6		
M-R0-PZ-4	4.0			6.0		
M-R50-PZ-1	3.8	3.8	0.1	4.3	5.0	0.6
M-R50-PZ-2	3.7			5.8		
M-R50-PZ-3	3.9			5.0		

Table 4 Results of UPV tests

Specimens	*S* (mm)	*T* (μs)	*V* (mm/μs)
M-R0-1	296	56.7	5.22
M-R0-2	296	55.6	5.32
M-R0-3	297	56.9	5.22
M-R0-4	297	56.5	5.26
M-R50-1	299	61.9	4.83
M-R50-2	295	60.8	4.85
M-R50-3	298	61.1	4.88
M-R50-4	298	60.8	4.90
M-R0-PZ-1	302	60.2	5.02
M-R0-PZ-2	300	59.3	5.06
M-R0-PZ-3	305	59.7	5.11
M-R0-PZ-4	300	59.8	5.02
M-R50-PZ-1	302	59.3	5.09
M-R50-PZ-2	302	63.2	4.78
M-R50-PZ-3	303	65.0	4.66
M-R50-PZ-4	302	64.7	4.67

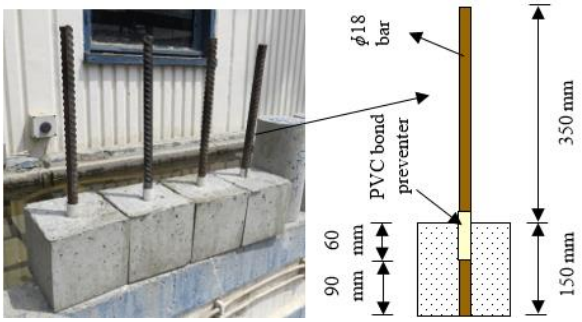

(a)

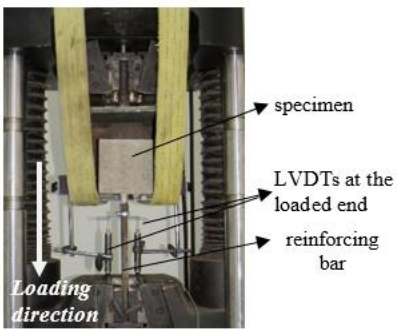

(b)

Fig. 9 Pull-out (a) Specimens, (b) Test set-up

UPV values are listed in Table 4. In this table, S, T and V refer to the distance between probes (mm), the duration of the ultrasonic waves pass through the specimen (μs) and the ultrasonic pulse velocity (mm/μs). According to Jones and Facaoaru (1969), the UPV values 3 mm/μs, 4 mm/μs and 5 mm/μs correspond to very poor quality, fair quality and very good quality in terms of strength and homogenity of concrete, respectively. According to the evaluation of UPV values, which were around 5 mm/μs, based on the study by Jones and Facaoaru (1969), the concrete mixtures used for the production of specimens presented very good concrete strength and do not contain extensive voids or cracks. According to the test results, UPV values decreased with the incorporation of RCA (7% decrease in group M-R50 with respect to the group M-R0), which can be explained by the increased porosity of RCA. The internal porosity causes a decrease in the wave propagation speed due to the dispersion of the waves around the voids. Incorporation of fly ash caused a slight decrease in the UPV values (4% decrease in the group M-R0-PZ with respect to the group M-R0, 2% decrease in the group M-R50-PZ with respect to group M-R50, 8% decrease in the group M-R0 with respect to group M-R50-PZ). A similar observation was reported by Kou *et al.* (2012) and De Brito *et al.* (2016) for concrete incorporating RCA, where RCA was obtained from normal strength concrete (50 MPa).

It should also be noted that the UPV values of M-R0-PZ is only 4% higher than that of M-R50. Similarly, the mechanical properties of M-R0-PZ and M-R50 are also quite close: the tensile strength values of M-R0-PZ is almost 5% higher than that of M-R50, while flexural and compressive strength values of M-R0-PZ are approximately 4% and 3% less than that of M-R50, respectively. These results indicate that UPV values and mechanical properties have quite similar trends. The pull-out tests were conducted on 150 mm×150 mm×150 mm cube specimens according to ASTM C234 (1991) (Fig. 9(a)). The ribbed steel rebars (S420 type), which were 500 mm in length and 18 mm in diameter, were embedded to the cube specimens before concrete casting. The stress-strain relationships of the deformed steel rebars are given in Fig. 10(a). The bond length was 90 mm (=5ϕ), and the rest of the specimen was debonded by the use of a PVC pipe (Fig. 9(a)). Two linear variable differential transducers (LVDTs) were attached to the bars for measuring concrete-rebar slip (Fig. 9(b)). While

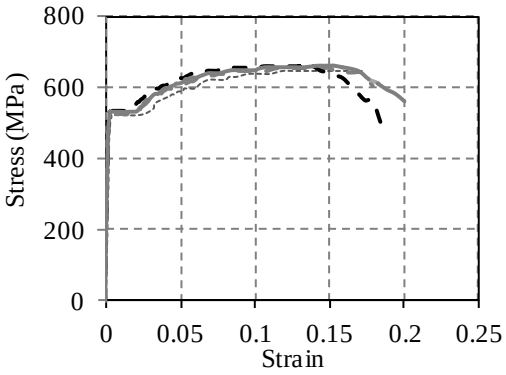

(a)

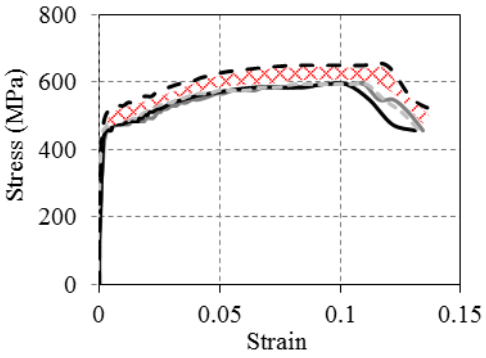

(b)

Fig. 10 Stress-strain relationships of (a) 18 mm steel rebars used in pull-out tests, (b) 8 mm steel rebars used in slabs

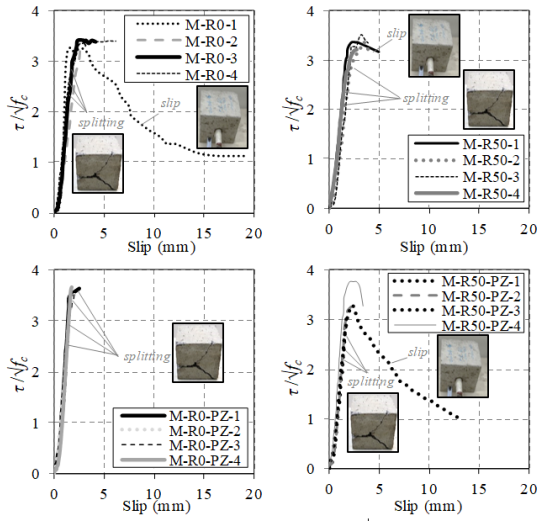

Fig. 11 Bond-slip relationships of the specimens

the failures of nine out of twelve specimens were governed by splitting, the failures of the rest of the specimens (one from each of the groups M-R0, M-R50 and M-R50-PZ) were governed by slip at around 2 mm (Fig. 11). In this figure, the bond stress ($\tau_b=F/\pi\Phi l_b$; F is the maximum pull-out load, ϕ is the diameter of the reinforcing bar, and lb is the bonded bar length) is normalized with concrete tension strength for eliminating the adverse effects of different concrete compressive strength of each concrete mix. As also seen in this figure, while most of the failures of the

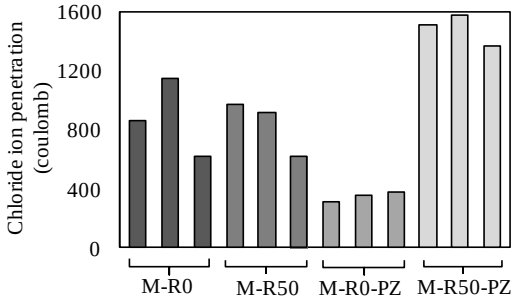

Fig. 12 Test results for chloride ion penetration

Fig. 13 Production of slabs

specimens were governed by splitting rather than slip, the bond strengths and splitting strengths of the specimens are similar. The local bond-slip relationship was evaluated considering the ratio between the bond stress and the square root of the compressive strength according to fib Model Code [72]. As also seen in Fig. 11, the ratio between the bond stress and the square root of the compressive strength were found to be greater than the value of 2.5. This indicates that the bond-slip models recommended by fib Model Code (2010) can safely be used for concrete made with RCA as well.

Moreover, to investigate the permeability of concrete

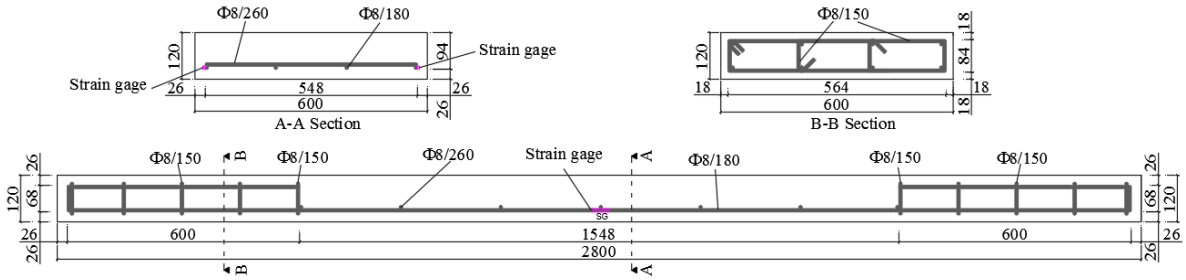

Fig. 14 Reinforcement cage of the slabs (Dimensions are in mm)

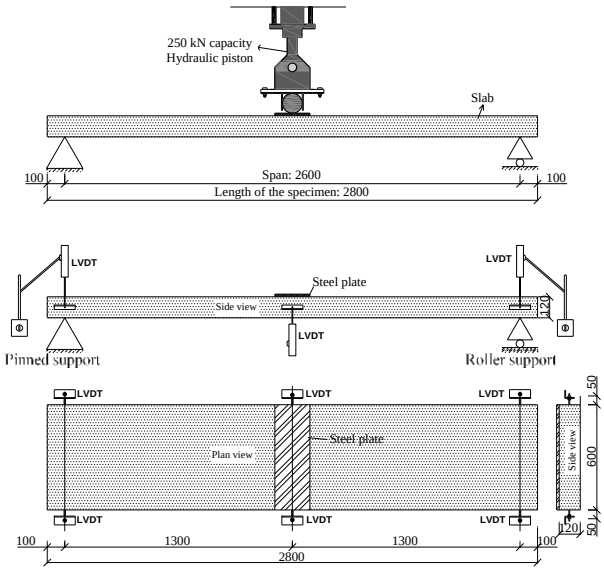

Fig. 15 Test setup (Dimensions are in mm)

mixtures incorporating NA and RCA with and without fly ash, rapid chloride penetration tests were carried out on 52 mm×100 mm cyclinder specimens according to ASTM C1202 (2017). Due to high permeability of the samples of the groups M-R0, M-R50 and M-R50-PZ, the temperature measured during the test increased above the limits indicated by ASTM C1202 (2017). Therefore, the test duration was modified to 1 hour instead of 6 hours, as recommended by ASTM C1202 (2017). The test results are presented in Fig. 12. As seen in this figure, the measured values of the specimens of the group M-R0 and the group M-R50 are similar. The incorporation of fly ash reduced the conductivity of the specimens of the group M-R0-PZ, where the measured values decreased 60% with respect to the specimens of the group M-R0 as already reported in literature (ASTM C1202 2017, Thomas and Wilson 2002). This reduction has been attributed to a refinement in the pore structure (Thomas 1989, Marsh *et al.* 1985). Furthermore, conductivity tests performed on mortar and cement paste have also indicated that fly ash reduces the chloride permeability (Page *et al.* 1981, Ngala *et al.* 1995, Thomas *et al.* 1995-1999, Bamforth 1999, Thomas 2004). Conversely, the incorporation of fly ash had negative impact on the specimens of the group M-R50-PZ, which resulted in an increase of 69% in the measured values of the specimens of this group with respect to the specimens of the group M-R50. The main reason for the increase in conductivity of the group M-R50-PZ is the reduction of the quality of interfacial transition zone (ITZ) around RCA particles. In concrete incorporating only NA, when fly ash is added, ITZ is so thin that it becomes denser due to finer particle size of fly ash and its reactions with the calcium hydroxide. However, due to thicker porous zones (old cement mortar) around RCA, fly ash particles are not as effective in densification by its fineness and reactivity with calcium hydroxide. On the contrary, since cement content is reduced when fly ash is added, the concrete permeability can be adversely affected.

2.3 Testing of slabs

Twelve full-scale one-way RC slabs were cast in dimensions of 2800 mm×600 mm×120 mm (span×width×thickness) (Fig. 13). Steel reinforcement cages were constructed using ϕ8 reinforcing bars. Clear concrete cover (distance from the outermost fiber of the longitudinal bars to the outermost fiber of concrete) is 26 mm. The stress-strain relationships of reinforcing bars used in the slabs are presented in Fig. 10(b). As seen in this figure, there is a variation, shown with a hatched area, in stress-strain relationships of the tested reinforcing bars. This variation is also considered during theoretical calculations. The reinforcement details of all slabs were the same and reinforcement ratio in longitudinal direction was 0.37% (Fig. 14). The slabs were subjected three-point bending test under monotonic increasing deflections until the failure load was reached (Fig. 15). Two out of six LVDTs were installed at mid-span, while the other four LVDTs were installed at supports. Two strain gages were also installed on the longitudinal reinforcing bars at the mid-span for observing the variations in strains during bending (Fig. 14).

Force-mid span deflection relationships and the average load-mid span deflection curves of the slabs are presented in Figs. 16 and 17(a), respectively. As seen from these figures, the slabs of the group M-R50 showed the lowest resistance among their counterparts (13% less load bearing capacity with respect to the slabs of the group M-R0), while the slabs of the group M-R0 showed the highest resistance. All slabs showed a remarkably ductile behavior after the maximum load was reached and maintained their strength up to large deflections until the reinforcing bars ruptured. According to the strain data obtained from the strain gages, the yielding of reinforcing bars was observed at and around mid span deflection of L/180 (L: Span) for all the groups of slabs. The first fine flexural cracks were observed at the mid span deflection of L/2000-L/3000 and the rupture of

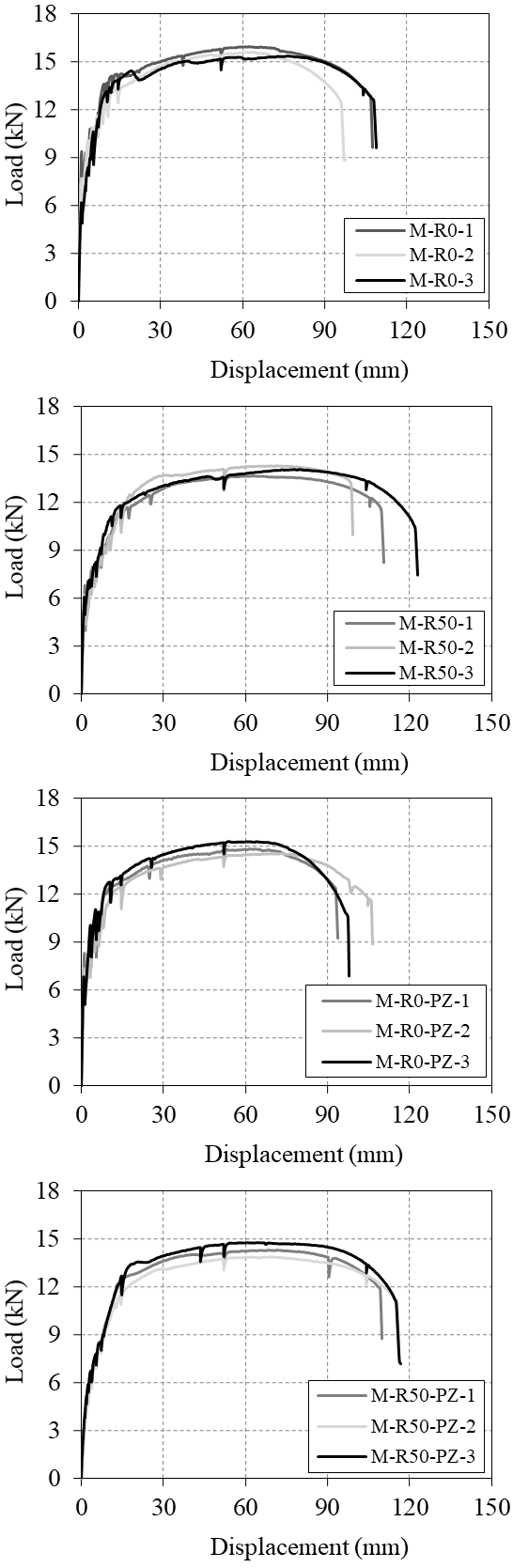

Fig. 16 Force-mid span deflection relationships of the slabs

reinforcing bars was observed in the mid span deflection of around L/25 for all the groups of slabs. It should be noted that prior to the rupture of reinforcing bars the maximum

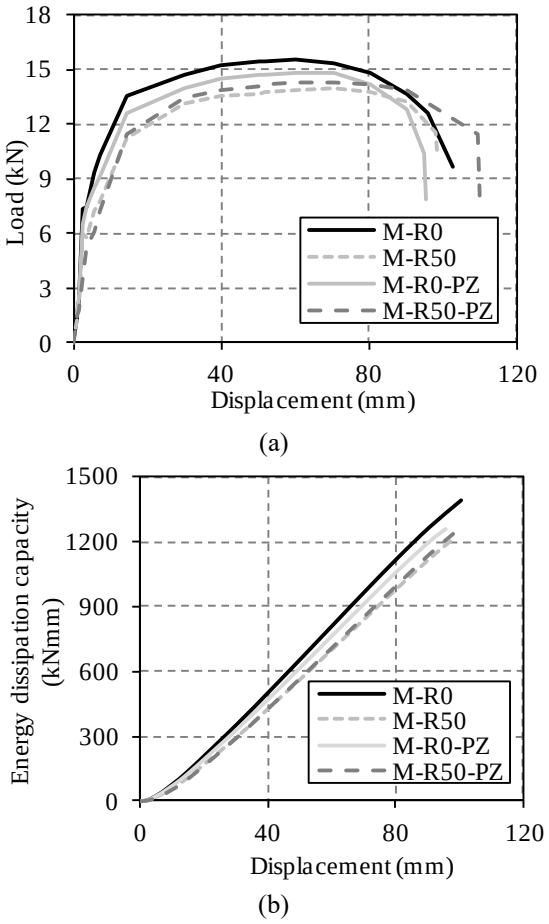

Fig. 17 (a) Average load-mid span deflection curves of the slabs, (b) Energy dissipation capacities of slabs (Average of each group)

strain value of reinforcing bars was measured to be approximately 5% from strain gages. Even at the utmost target mid span deflection, no concrete crushing was observed at the compression zone. The visual observations of progressive damage to the slabs during testing and the markings of the cracks on the slabs are shown in Fig. 18. It is worth to note that the evolution of damage was similar for all of the slabs. During the autopsy after the tests, the cover concrete was removed and the yielding and rupture of steel reinforcing bars were clearly observed (Fig. 19).

The energy dissipation capacity is defined as the area under the corresponding average load-mid span deflection curve at each loading step and presented in Fig. 17(b). As seen in this figure, the energy dissipated by the slabs of the group M-R0 is only slightly higher (varying between 4%-7%) than the other tested slabs due to its slightly higher strength and stiffness with respect to the other tested slabs as seen in Fig. 17(a).

3. Numerical study

The slab was modelled using finite element method to obtain the theoretical nonlinear lateral load-mid span deflection relationships of the specimens. Inelastic deformations of the slab were taken into account by a

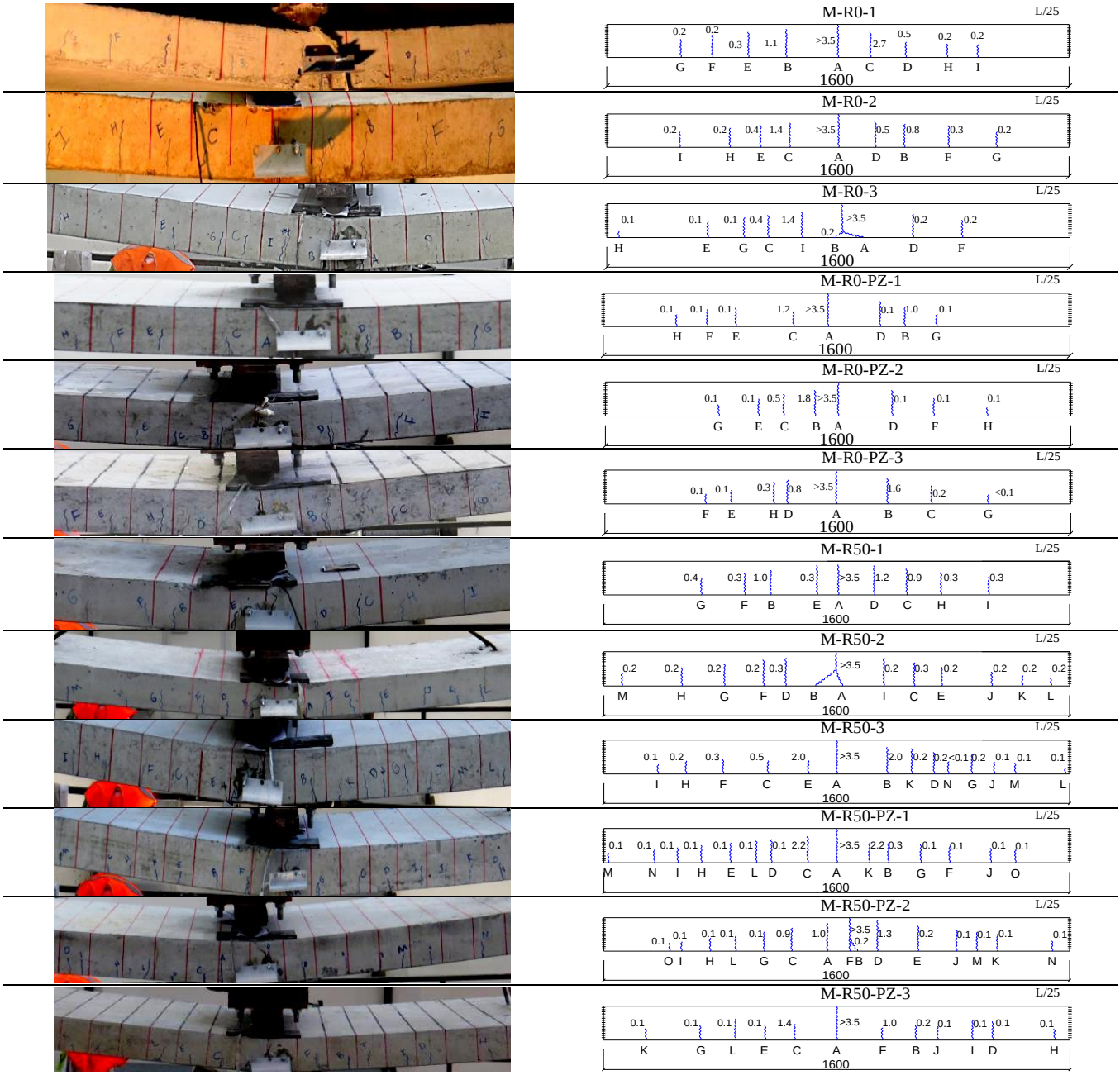

Fig. 18 Crack distribution during testing of the slabs

plastic hinge located at the maximum moment zone (at the mid span). As the first step, the nonlinear moment-curvature relationships of the critical cross-sections (span and support sections) of the slabs were obtained through a fiber-analysis approach using the XTRACT 3.0.8 computer program. In the moment-curvature analysis, the stress-strain relationship of concrete in compression was modelled considering the compression test results carried out on standard cylinders (Fig. 20(a)). Steel reinforcing bars in tension were assumed to behave in an elastic-plastic manner with strain hardening based on tension tests on reinforcing bars (Fig. 20(b)). It is worth highlighting that, rather than the compression strength of concrete, the amount and mechanical characteristics of the reinforcing steel dominate the load bearing capacity and ductility of the slabs. Therefore, defining the stress-strain relationship of the steel reinforcing bar has significant effect for realistic prediction of the load bearing and deformation capacity. For this purpose, as aforementioned, the variation in stress-strain relationships of the tested reinforcing bars was considered by the lower and upper bounds shown in Figs. 10(b) and 20(b). Sequentially, the plastic-hinge rotations were obtained by multiplying the section curvatures by the length of the plastic hinge, which was assumed to be equal to the thickness of the slab (h) considering the recommendation given in the Turkish Seismic Design Code (2017). It should be noted that the equations proposed by Baker (1956) and Mattock (1967) give the values of 1.2h and 0.9h, respectively. As a last step, a nonlinear analysis was executed for the slab model. For the analysis, the nonlinear behavior was assumed to occur within the frame element at the concentrated plastic hinge. The analysis consists of

(a)

(b)

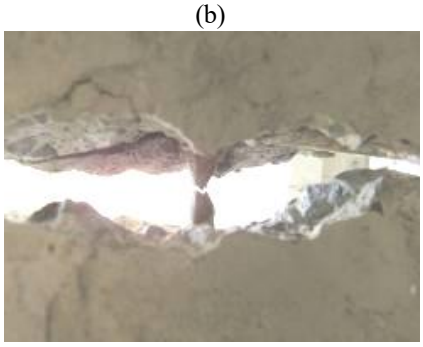

(c)

Fig. 19 Autopsy (a) Removal of concrete cover, (b) Yielding of reinforcing bar in longitudinal direction, (c) Rupture of reinforcing bar

vertical load pattern, and an incremental event-by-event analysis in which the load pattern is applied through increments corresponded to stiffness changes in the structural element. During the analysis, maximum total steps per stage, maximum events per step, iteration convergence relative tolerance were taken as 200, 24, and 0.0001, respectively. The first load step consists of an elastic analysis of the structural element. The loads were scaled to a level corresponded to the achievement of the first discontinuity in the load-displacement response. Thereby, the first hinge was created in the structural element. For the next load increment, the stiffness of the structural element was modified, and another elastic analysis was performed. At this step, the incremental loads were also scaled to a level to be corresponded to the achievement of the next discontinuity in the load-displacement response in the structural element. This algorithm was continued until the displacement of the structural element reached to the target displacement. The theoretically obtained load-deflection relationships are presented in Fig. 21 together with the experimentally

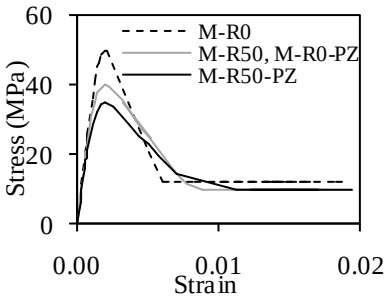

(a)

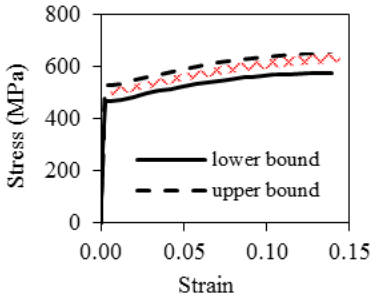

(b)

Fig. 20 The mechanical characteristics of (a) Concrete, (b) Longitudinal steel reinforcing bars taken into account during numerical analysis, Note: Since the groups M-R50 and M-R0-PZ had similar concrete compressive strength, the concrete stress-strain relationship of these groups are presented on a single curve

obtained load-deflection relationships. As seen in this figure, an adequate correlation was achieved between the experimentally and the theoretically obtained load-deflection relationships. This result shows that the conventional RC theory remains valid for the slabs incorporating RCA sourced from low strength concrete. The comparison of the theoretical predictions and the test results also showed that for the same design moment, approximately the same amount of reinforcing bar is needed for the slabs incorporating NA and RCA at approximately same compressive strengths.

For the comparison of the experimentally observed and theoretically predicted damage development and failure modes, the stress-strain relationships of concrete at the extreme compression fiber and tensile reinforcing bars and the moment-curvature relationships at the plastic hinge zone are presented in Figs. 22-24. In these figures, two steel stress-strain relationships are presented for representing the variation in stress-strain relationships of the tested reinforcing bars (Figs. 10(b) and 20(b)). ε_{s-l} and ε_{s-u} refer to the tensile strains of reinforcing bars corresponding to lower and upper bounds of stress-strain relationships. ε_{c-l} and ε_{c-u} refer to the compressive strains of concrete, which were obtained when stress-strain relationships of reinforcing bars with lower and upper bounds are used. Likewise, σ_{c-l} and σ_{c-u} refer to compressive stresses of concrete, which were obtained when stress-strain relationships of reinforcing bars with lower and upper bounds are utilized. In these figures, the numerical moment-curvature relationships are also shown for the slab sections

Table 5 Damage limits in terms of steel tensile strains (TSDC 2007)

Level	Damage limits	Limit for reinforcement strain	Upper limit for concrete strain
A	Minimum damage	0.01	0.0035 for ε_c
B	Moderate damage	0.04	0.0035 + 0.01 (ρ_s /ρ_{sm}) ≤ 0.0135 for ε_{cc}
C	Heavy damage	0.06	0.004 + 0.014 (ρ_s /ρ_{sm}) ≤ 0.018 for ε_{cc}

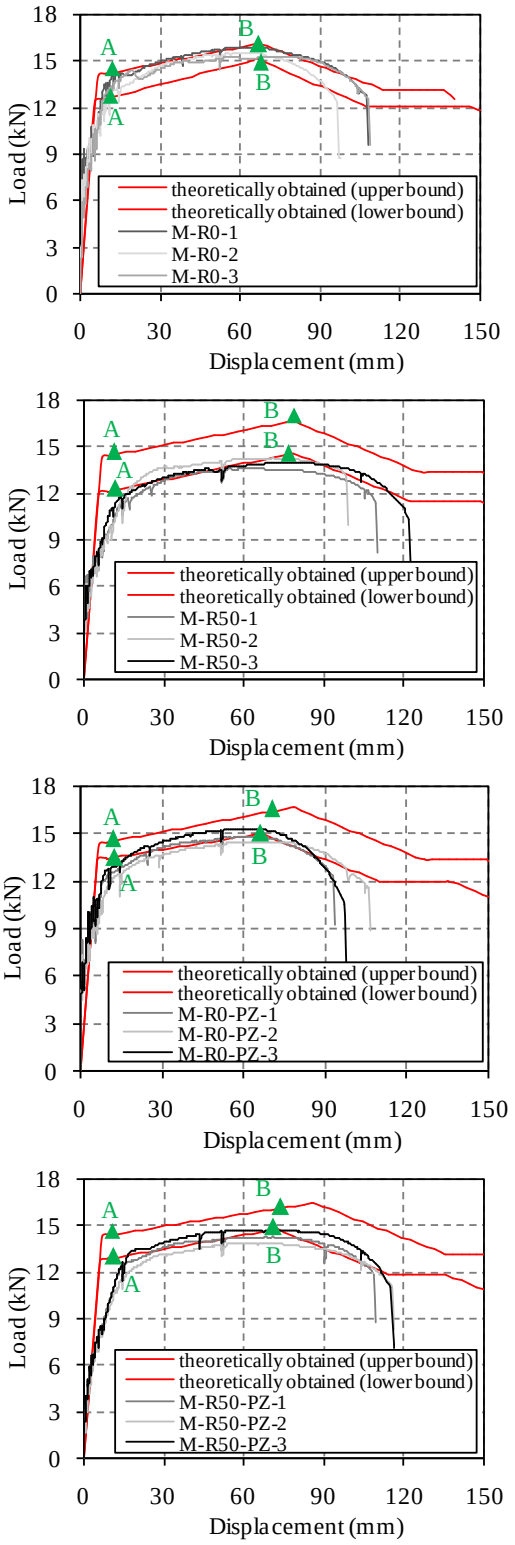

Fig. 21 Force-mid span deflection relationships of the slabs

using actual material characteristics. As seen in these figures, the values of moments and strains are given for three levels, namely A, B and C. These points correspond to different structural performance levels of the slabs such as minimum damage, moderate damage and heavy damage as stated in Turkish Seismic Design Code (2017) and Table 5. In Table 5, εc and εcc are the concrete strain at the extreme compression fiber for unconfined and confined concrete, respectively, and ρs and ρsm represent the existing and the required volumetric ratios of transverse reinforcement, respectively. It should be noted that since the slabs of the groups M-R50 and M-R0-PZ had similar concrete compressive strength, their theoretical calculations are presented in the same figure (Fig. 23). For ultimate steel strain at collapse level, εs is set to 0.06 in Turkish Seismic Design Code (2007) (Table 5). However, at this εs level, the steel strains in tension passed beyond the measurement capacity of the straingages. Therefore, the values at point C correspond to εs value of 0.05. As aforementioned, the damage progression of the slabs started with the yielding of reinforcing bar and followed by the rupture of reinforcing bar. Meanwhile, no concrete crushing was observed. However, according to the theoretically obtained damage proggession, the slabs failed in a progressive manner: yielding of reinforcing bar (at the time of yielding of reinforcing bar εc was observed to be around 0.006), crushing of concrete and finally rupture of reinforcing bar. The comparison of Fig. 21 and Figs. 22-24 imply that the load bearing capacities and failure mechanisms of the slabs can be predicted through thereoretical calculations with a reasonable accuracy up to very high displacement levels by the presented algorithm.

4. Conclusions

In this study, the viability of using RCA sourced from low strength concrete for substituting NA was investigated for RC structural members. Based on the experimental and numerical analysis, the following conclusions can be drawn:

- The compression strength of concrete decreased slightly with the incorporation of RCA and fly ash.
- The incorporation of RCA and fly ash caused a decrease in flexural strengths.
- The results of splitting tensile tests showed that the incorporation of RCA and fly ash reduced the splitting tensile strength.
- The pull-out test showed that bond-slip behaviors of concretes made with NA and RCA are similar. It is also shown that the bond-slip models recommended by fib Model Code (2010) can safely be used for determination of bond strength of concrete made with RCA as well.
- The full-scale bending tests indicated that all slabs showed a remarkably ductile behavior after the maximum load was reached and maintained their strengths up to large deflections until the reinforcing bars ruptured. The load carrying capacities and evolution of damage of all slabs were similar regardless of incorporation of RCA and fly ash. Likewise, there was only marginal difference in energy dissipation capacities of the slabs.

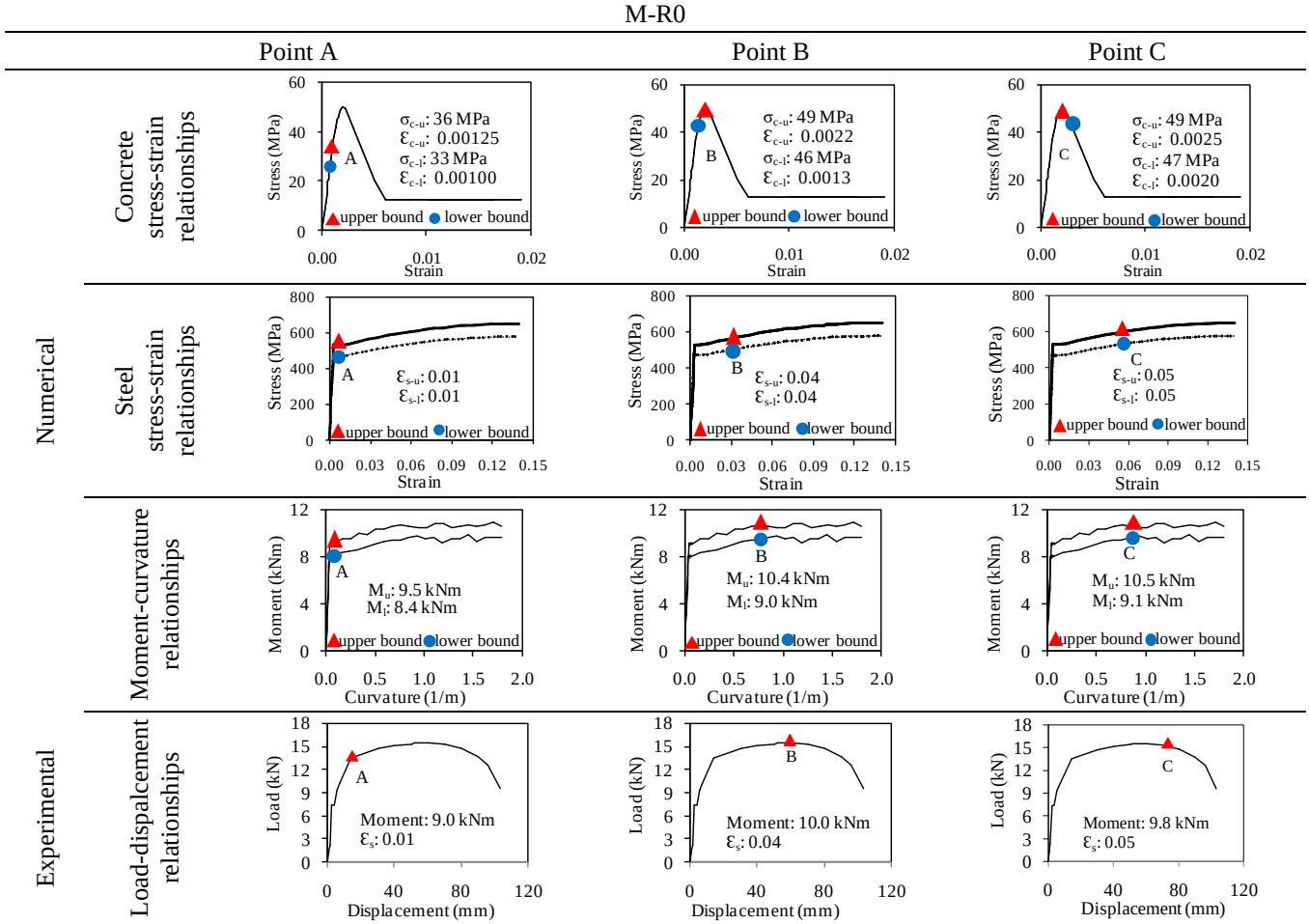

Fig. 22 Moment-curvature and stress-strain relationships for the slabs of the group M-R0

• The experimentally and the theoretically obtained load-deflection relationships were found to be compatible up to high displacement levels. Since the theoretical load-deflection relationships were obtained through conventional RC theory, plastic hinge concept and fiber analysis approach, it is clear that the conventional RC theory remains valid for the slabs incorporating RCA sourced from low strength concrete.

It should be emphasized that all findings are valid for the ranges of the parameters tested within this study. Although the slabs generally work under gravity loads, they are exposed to reversed cylic loads, particularly, inplane diaphram forces during earthquakes. Therefore, further investigations should be carried out to generalize and validate the presented findings for other cases and pave the way for the use of larger amount of RCA to obtain further environmental and economical benefits.

Acknowledgments

This study is supported by The Scientific and Technological Research Council of Turkey under grant number 115M029. The supports of O. Manzak, Yapı Merkezi and Akçansa Companies are gratefully acknowledged. The invaluable contributions of staff of ITU Structural and Earthquake Engineering and ITU Infrastructure Materials Laboratories are acknowledged. The authors are thankful to L. Bank and A. Yazdanbakhsh from City College of New York for their valuable advices. The authors are also thankful to the supports of B. Aldirmaz, C. Cakmakli and F. Gultekin.

References

Ajdukiewicz, A. and Kliszczewicz, A. (2002), "Influence of recycled aggregates on mechanical properties of HS/HPC", *Cement Concrete Comp.*, **24**(2), 269-279.

ASTM C114-05 (2005), *Standard Test Methods for Chemical Analysis of Hydraulic Cement*, ASTM International, West Conshohocken, Pennsylvania, U.S.A.

ASTM C1202 (2017), *Standard Test Method for Electrical Indication of Concrete's Ability to Resist Chloride Ion Penetration*, ASTM International, West Conshohocken, Pennsylvania, U.S.A.

ASTM C1260 (2014), *Standard Test Method for Potential Alkali Reactivity of Aggregates (Mortar-Bar Method)*, ASTM International, West Conshohocken, Pennsylvania, U.S.A.

ASTM C234 (1991), *Standard Test Method for Comparing Concretes on the Basis of the Bond Developed with Reinforcing Steel*, ASTM International, West Conshohocken, Pennsylvania, U.S.A.

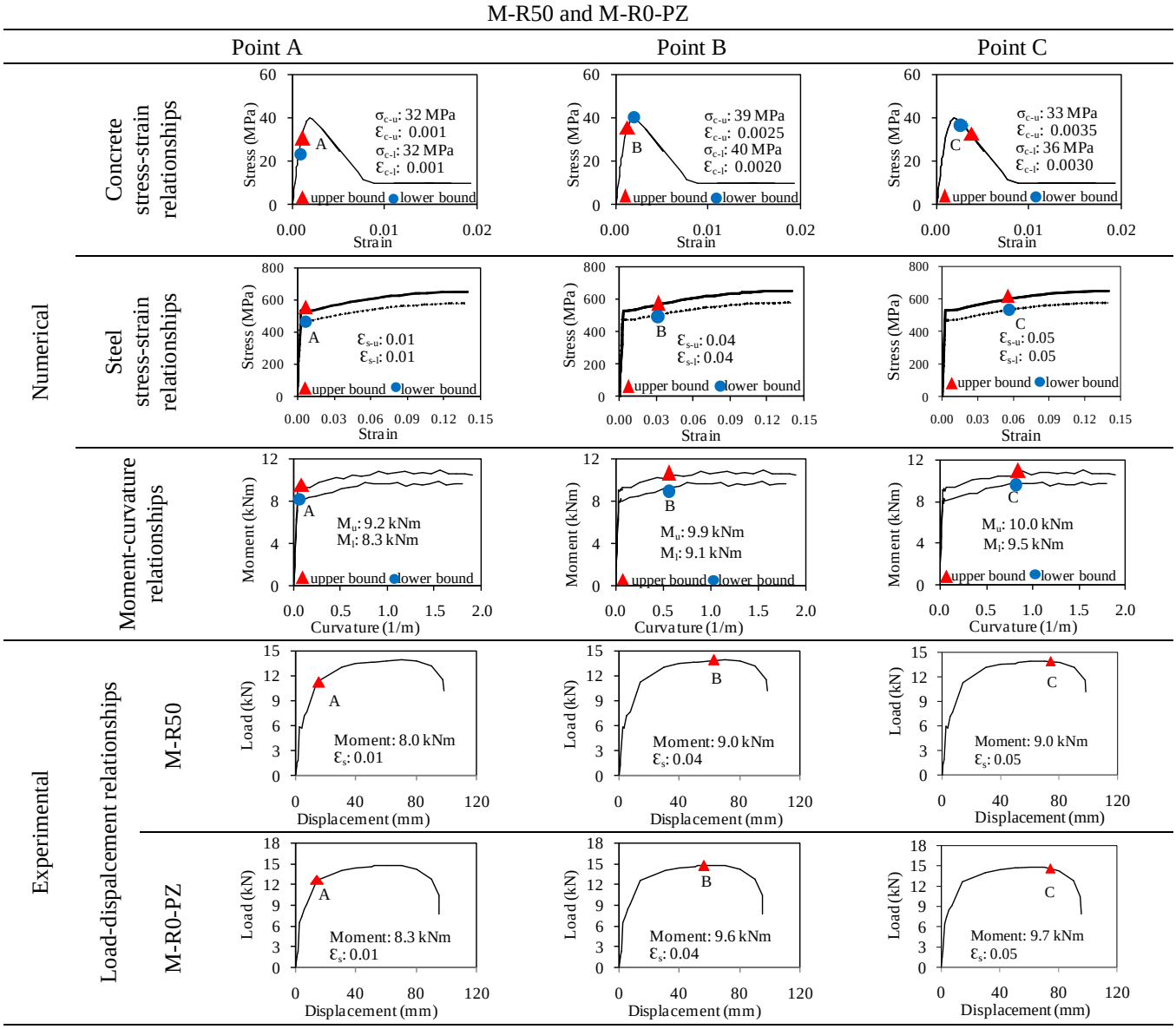

Fig. 23 Moment-curvature and stress-strain relationships for the slabs of the groups M-R50 and M-R0-PZ

ASTM D422-63 (2007), *Standard Test Method for Particle-Size Analysis of Soils*, ASTM International, West Conshohocken, PA.ASTM C597 (2002), *Standard Test Method for Pulse Velocity through Concrete*, ASTM International, West Conshohocken, Pennsylvania, U.S.A.

Attaullah, S., Irfan, U., Raza U.K and Ehsan, U.Q. (2013), "Experimental investigation on the use of recycled aggregates in producing concrete", *Struc. Eng. Mech.*, **47**(4), 545-557.

Baker, A. (1956), *Ultimate Load Theory Applied to the Design of Reinforced and Prestressed Concrete Frames*, Concrete Publications Ltd., London, U.K.

Bamforth, P.M. (1999), "The derivation of input data for modelling chloride ingress from eight-year uk coastal exposure trials", *Mag. Conc. Res.*, **51**(2), 87-96.

Corinaldesi, V. (2010), "Mechanical and elastic behaviour of concretes made of recycled-concrete coarse aggregates", *Constr. Build. Mater.*, **24**(9), 1616-1620.

Cosgun, C., Comert, M., Demir, C. and Ilki, A. (2012), "FRP retrofit of a full-scale 3D RC frame", *Proceedings of the 6th International Conference on Fibre-Reinforced Polymer (FRP) Composites in Civil Engineering*, Rome, Italy.

De Brito, J., Ferreira, J., Pacheco, J., Soares, D. and Guerreiro, M. (2016), "Structural, material, mechanical and durability properties and behaviour of recycled aggregates concrete", *J. Build. Eng.*, 61-16.

Fathifazl, G., Fazaqpur, A.G., Isgor, O.B., Abbas, A., Fournier, B. and Foo, S. (2011), "Creep and drying shrinkage characteristics of concrete produced with coarse recycled concrete aggregate", *Cement Concrete Comp.*, **33**(10), 1026-1037.

Fathifazl, G. and Razaqpur, A.G. (2013), "Creep rheological models for recycled aggregate concrete", *ACI Mater. J.*, **110**(2), 115-126.

fib (Fédération International du Béton/International Federation for Structural Concrete), (2010), *Model Code 2010*, Lausanne, Switzerland.

Francesconi, L., Pani, L. and Stochino, F. (2016), "Punching shear strength of reinforced recycled concrete slabs", *Constr. Build. Mater.*, **127**, 248-263.

Garg, P., Singh, H. and Walia, B.S. (2013), "Optimum size of recycled aggregate", *GE-Int. J. Eng. Res.*, 35-41.

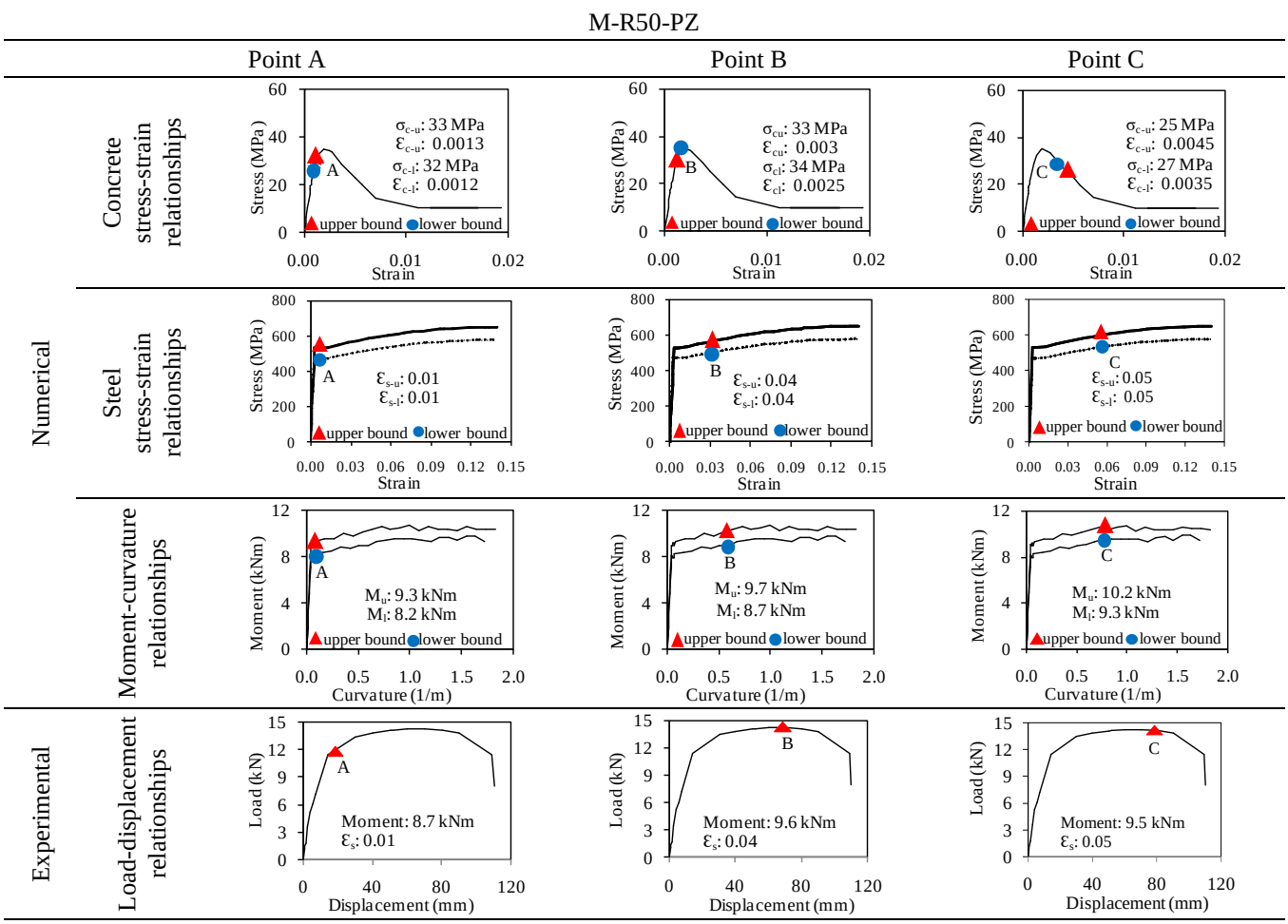

Fig. 24 Moment-curvature and stress-strain relationships for the slabs of the group M-R50-PZ

Ghatte, H.F., Comert, M., Demir, C. and Ilki, A. (2016), "Evaluation of FRP confinement models for substandard rectangular RC columns based on full-scale reversed cyclic lateral loading tests in strong and weak directions", *Polym.*, **8**(323), 1-24.

Gomez, J.M.V. (2002a), "Shrinkage of concrete with replacement of aggregate with recycled concrete aggregate", *ACI Spec. Publ.*, **209**, 475-496.

Gomez, J.M.V. (2002b), "Creep of concrete with substitution of normal aggregate by recycled concrete aggregate", *ACI Spec. Publ.*, **209**, 461-474.

Gonçalves, P. and De Brito, J. (2009), "Recycled aggregate concrete (RAC)-comparative analysis of existing specifications", *Mag. Concrete Res.*

Hansen, T.C. (1992), *Recycling of Demolished Concrete and Masonry*, E&FN SPON, London, U.K.

Hasan, N.K., Nasim, K.S. and Khaled, H.H. (2017), "Effect of silica fume on mechanical properties of concrete containing recycled asphalt pavement", *Struct. Eng. Mech.*, **62**(3), 357-364.

Henschen, J., Teramoto, A. And Lange, D.A. (2012), "Shrinkage and creep performance of recycled aggregate concrete", *Proceedings of the 7th RILEM International Conference on Cracking in Pavements*, the Netherlands.

Ho, N.Y., Lee, Y.P.K., Lim, W.F., Zayed, T., Chew, K.C., Low, G.L. and Ting, S.K. (2013), "Efficient utilization of recyceled concrete aggregate in structural concrete", *J. Mat. Civil Eng.*, **25**(3), 318-327.

Ilki, A. And Celep, Z. (2012), "Earthquakes, existing buildings, and seismic design codes in Turkey", *Arab. J. Sci. Eng.*, **37**(2), 365-380.

Jones, R. and Facaoaru, I. (1969), "Recommendations for testing concrete by the ultrasonic pulse method", *Mat. Str.* (RILEM) **2**(10), 275-284.

Khalaf, F.M. and DeVenny, A.S. (2004), "Recycling of demolished masonry rubble as coarse aggregate in concrete: Review", *ASCE J. Mater. Civil Eng.*, **16**(4), 331-340.

Kou, S.C., Poon, C.S. and Wan, H.W. (2012), "Properties of concrete prepared with low-grade recycled aggregates", *Constr. Build. Mater.*, **36**, 881-889.

Limbachiya, M.C., Koulouris, A., Roberts, J.J. and Fried, A.N. (2004), "Performance of recycled concrete aggregate", *Proceedings of the International Symposium on Environmental-Conscious Materials and Systems for Sustainable Development*, Koriyama, Japan.

Lopez-Gayarre, F., Serna, P., Domingo-Cabo, A., Serrano-Lopez, M.A. and Lopez-Colina, C. (2009), "Influence of recycled aggregate quality and proportioning criteria on recycled concrete properties", *Waste Mng.*, **29**(12), 3022-3028.

Malesev, M., Radonjanin, V. and Marinkovic, S. (2010), "Recycled concrete as aggregate for structural concrete production", *Sustainab.*, **2**(5), 1204-1225.

Marceau, M.L., Gajda, J. and Van Geem, M.G. (2002), *Use of Fly Ash in Concrete: Normal and High Volume Ranges*, PCA R&D Serial No. 2604, Portland Cement Association, Skokie, Illinois.

Marsh, B.K., Day R.L. and Bonner, D.G. (1985), "Pore structure characteristics affecting the permeability of cement paste containing fly ash", *Cement Concrete Res.*, **15**(6), 1027-1038.

Mattock, A.H. (1967), "Discussion of 'rotational capacity of reinforced concrete beams", *J. Struct. Div.*, **93**(ST2), 519-522.

Michaud, K., Hoult, N., Lotfy, A. and Lum, P. (2016), "Performance in shear of reinforced concrete slabs containing recycled concrete aggregate", *Mater. Struct.*, **49**(10), 4425-4438.

Ngala, V.T., Page, C.L., Parrott L.J. and Yu, S.W. (1995), "Diffusion in cementitious materials: ii further investigations of chloride and oxygen diffusion in well-cured opc and opc/30%pfa pastes", *Cement Concrete Res.*, **25**(4) 819-826.

Pacheco Torgal, F., Tam, V.W.Y., Labrincha, J.A., Ding Y. and De Brito, J. (2013), *Handbook of Recycled Concrete and Demolition Waste*, Woodhead Publishing Limited.

Page, C.L., Short, N.R. and El Tarras, A. (1981), "Diffusion of chloride ions in hardened cement pastes", *Cement Concrete Res.*, **11**(3) 395-406.

Palaniraj, S. and Dhinakaran, G. (2013), "Durability characteristics of recycled aggregate concrete", *Struct. Eng. Mech.*, **47**(5), 705-711.

Poon, C.S., Shui, Z.H. and Lam, L. (2004), "Effect of microstructure of ITZ on compressive strength of concrete prepared with recycled aggregates", *Constr. Build. Mater.*, **18**(6), 461-468.

Rahal, K. (2007), "Mechanical properties of concrete with recycled coarse aggregate", *Build. Environ.*, **42**(1), 407-415.

Rakshvir, M. and Barai, S.V. (2006), "Studies on recycled aggregates based concrete", *Waste Mng. Res.*, **24**(3), 225-233.

Rao, H.S., Reddy, V.S.K. and Ghorpade, V.G. (2012), "Influence of recycled coarse aggregate on punching behaviour of recycled coarse aggregate concrete slabs", *Int. J. Mod. Eng. Res.*, **2**(4), 2815-2820.

Rao, M.C., Bhattacharyya, S.K. and Barai, S.V. (2011), "Influence of field recycled coarse aggregate on properties of concrete", *Mater. Struct.*, **44**(1), 205-220.

Rise, N., De Brito, J., Correia, J.R. and Arruda, M.R.T. (2015), "Punching behaviour of concrete slabs incorporating coarse recycled concrete aggregates", *Eng. Struct.*, **100**, 238-248.

Sanchez, M. and Gutierrez, P.A. (2004), "Influence of recycled aggregate quality on concrete properties", *Proceeding of the International RILEM Conference: The Use of Recycled Materials in Building and Structures*, Barcelona, Spain.

Schubert, S., Hoffmann, C., Leemann, A., Moser, K. and Motavalli, M. (2012), "Recycled aggregate concrete: Experimental shear resistance of slabs without shear reinforcement", *Eng. Struct.*, **41**, 490-497.

Shayan, A. And Xu, A. (2003), "Performance and properties of structural concrete made with recycled concrete aggregate", *ACI Mat. J.*, **100**(5), 371-380.

Silva, R.V., DeBrito, J. and Dhir, R.K. (2015), "Prediction of the shrinkage behavior of recycled aggregate concrete: A review", *Constr. Build. Mater.*, **77**, 327-339.

Sim, J. and Park, C. (2011), "Compressive strength and resistance to chloride ion penetration and carbonation of recycled aggregate concrete with varying amount of fly ash and fine recycled aggregate", *Waste Mng.*, **31**(11), 2352-2360.

Tangchirapat, W., Buranasing, R. and Jaturapitakkul, C. (2010), "Use of high fineness of fly ash to improve properties of recycled aggregate concrete", *J. Mater. Civil Eng.*, **22**(6), 565-571.

Tapan, M., Comert, M., Demir, C., Sayan, Y., Orakcal, K. and Ilki, A. (2013), "Failures of structures during the October 23, 2011 Tabanlı (Van) and November 9, 2011 Edremit (Van) earthquakes in Turkey", *Eng. Fail. Analy.*, **34**, 606-628.

Thomas, C., Setien, J. and Polanco, J.A. (2016), "Structural recycled aggregate concrete made with precast wastes", *Constr. Build. Mater.*, **114**, 536-546.

Thomas, M. (2007), *Optimizing the Use of Fly Ash in Concrete*, PCA, 24.

Thomas, M.D.A. (1989), "The effect of curing on the hydration and pore structure of hardened cement paste containing pulverized-fuel ash", *Adv. Cement Res.*, **2**(8), 181-188

Thomas, M.D.A. (2004), *Prevention of Reinforcement Corrosion in Concrete Structures. Part i: Carbonation-Induced Corrosion*, Canadian Civil Engineer: Special Issue on Durability of Concrete Structures, 22-25.

Thomas, M.D.A., Mukherjee, P.K., Sato, J.A. and Everitt, M.F. (1995), "Effect of fly ash composition on thermal cracking in concrete", *Proceedings of the 5th CANMET/ACI International Conference on Fly Ash, Silica Fume, Slag and Natural Pozzolans in Concrete*, ACI SP-153, American Concrete Institute, Detroit, Michigan, U.S.A.

Thomas, M.D.A., Shehata, M. and Shashiprakash, S.G. (1999), "The use of fly ash in concrete: Classification by composition", *Cement Concrete Agg.*, **12**(2), 105-110.

Thomas, M.D.A. and Wilson, M.L. (2002), *Supplementary Cementing Materials for Use in Concrete*, CD038, PCA, Skokie, IL.

TS EN 1097-2 (2010), *Tests for Mechanical and Physical Properties of Aggregates-Part 2: Methods for the Determination of Resistance to Fragmentation*, Turkish Standards Institute, Ankara, Turkey.

TS EN 1097-6 (2013), *Tests for Mechanical and Physical Properties of Aggregates-Part 6: Determination of Particle Density and Water Absorption*, Turkish Standards Institute, Ankara, Turkey.

TS EN 12390-3 (2002), *Testing Hardened Concrete-Part 3: Compressive Strength of Test Specimens*, Turkish Standards Institute, Ankara, Turkey.

TS EN 12390-5 (2002), *Testing Hardened Concrete-Part 5: Flexural Strength of Test Specimens*, Turkish Standards Institute, Ankara, Turkey.

TS EN 12390-6 (2002), *Testing Hardened Concrete-Part 6: Tensile Splitting Strength of Test Specimens*, Turkish Standards Institute, Ankara, Turkey.

TS EN 1367-2 (2011), *Tests for Thermal and Weathering Properties of Aggregates-Part 2: Magnesium Sulfate Test*, Turkish Standards Institute, Ankara, Turkey.

TS EN 1367-4 (2009), *Tests for Thermal and Weathering Properties of Aggregates Part 4: Determination of Drying Shrinkage*, Turkish Standards Institute, Ankara, Turkey.

TS EN 1744-1 (2013), *Tests for Chemical Properties of Aggregates-Part 1: Chemical Analysis*, Turkish Standards Institute, Ankara, Turkey.

TS EN 933-1 (2012), *Tests for Geometrical Properties of Agregates-Part 1: Determination of Particle Size Distribution Sieving Method*, Turkish Standards Institute, Ankara, Turkey.

TS EN 933-3 (2012), *Test for Geometrical Properties of Aggregates-Part 2: Determination of Particle Size Distribution-Test Sieves, Nominal Size of Apartures*, Turkish Standards Institute, Ankara, Turkey.

TS EN 933-4 (2009), *Tests for Geometrical Properties of Aggregates-Part 4: Determination of Particle Shape - Shape Index*, Turkish Standards Institute, Ankara, Turkey.

TS EN 933-9 (2010), *Tests for geometrical properties of aggregates-Part 9: Assessment of fines - methylene blue test*, Turkish Standards Institute, Ankara, Turkey.

Turkish Seismic Design Code (TSDC) (2017), *Regulations for Buildings to be Constructed in Earthquake Prone Areas*, Ankara, Turkey.

Urban Transformation Act, 06/05/2012–6306 (2012), *The Law of Transformation of Areas Under the Disaster Risk*, Republic of Turkey Ministry of Environment and Urbanization, Ankara, Turkey.

Vyas, C.M. and Bhatt, D.R. (2013), "Evaluation of modulus of

elasticity for recycled coarse aggregate concrete", *Int. J. Eng. Sci. Innov. Technol.*, **2**(1), 26.
Xiao, J., Li, L., Tam, V.W. and Li, H. (2014), "The state of the art regarding the long-term properties of recycled aggregate concrete", *Struct. Conc.*, **15**(1), 3-12.
Xiao, J., Li, W., Sun, Z. and Shah, S.P. (2012), "Crack propagation in recycled aggregate concrete under uniaxial compressive loading, *ACI Mater. J.*, **109**(4), 451-462.
Xiao, J., Sun, C. And Jiang, X. (2015), "Flexural behaviour of recycled aggregate concrete graded slabs", *Struct. Concrete*, **16**(2), 249-261.
XTRACT 3.0.8 (Computer software), Rancho Cordova, CA, TRC.
Yang, K.H., Chung, H.S. and Ashour, A. (2008), "Influence of type and replacement level of recycled aggregates on concrete properties", *ACI Mater. J.*, **3**, 289-296.
Yehia, S., Khan, S. and Abudayyeh, O. (2008), "Evaluation of mechanical properties of recycled aggregate for structural applications", *HBRC J.*, **4**(3), 7-16.
Zhou, J.H., Wang, X.B. and Yu, T.H. (2008), "Mechanic behavior test on recycled concrete simply-supported rectangular slabs", *J. Shenyang Jianzhu Univ. Nat. Sci.*, **24**(3), 41-415.

CC